Experimental study and thermodynamic modelling of the Ag-Cd-In system

Evelyne Fischer, K. Gajavalli, Georges Mikaelian, Benigni P., J. Rogez, A. Decreton, M. Barrachin

Experimental Study and Thermodynamic Modeling of the Ag-Cd-In System

E. Fischer[(1)], K. Gajavalli[(2)], G. Mikaelian[(3)], P. Benigni[(3)], J. Rogez[(3)], A. Decreton[(2)], M. Barrachin[(2)]

(1) Univ. Grenoble Alpes, CNRS, Grenoble INP, SIMAP, CMTC, F-38000 Grenoble, France

(2) Institut de Radioprotection et Sûreté Nucléaire, PSN-RES, SAG, LETR, Saint Paul les Durance cedex, France

(3) Aix Marseille Univ., Université de Toulon, CNRS, IM2NP, Marseille, France

Abstract

In the case of a severe accident, the silver-indium-cadmium alloy which constitutes the absorber rods of a pressurized water reactor is liable to melt, interact with other materials as fuel cladding and then provoke early degradation of the core. The control rod elements also interact with fission products (in particular iodine), and may significantly affect their speciation and transport in the primary circuit as well as their behavior in the containment. The knowledge of the Ag-Cd-In ternary phase diagram is therefore of great importance to estimate the potential release of the absorber elements from the core. In this work, the thermodynamic modeling of the ternary Ag-Cd-In system has been carried out using the CALPHAD approach, based on available experimental data for phase diagram and thermodynamic properties. It takes into account additional experimental data related in particular to the liquidus temperatures in cadmium-rich region which are reported in this paper. A set of self-consistent thermodynamic parameters was optimized by the least-squares method using the TERGSS program [1]. A satisfactory agreement was obtained between the experimental data and the calculated results.

Keywords: Ag-Cd-In; Thermodynamics; Modeling; CALPHAD

1. Introduction

The 80 wt.% Ag, 15 wt.% In, 5 wt.% Cd alloy (SIC alloy) is used as absorber material in most of the PWR reactors. During a severe accident (i.e. loss of cooling), the SIC alloys start to melt at 1016 K [2]. This does not induce any core degradation as long as the molten alloy remains inside the stainless steel cladding of the absorber rod. As the temperature increases, cadmium vapor and helium initially present in the rod cause internal pressurization (in a low-pressure scenario) until the rupture of the absorber rod stainless steel cladding. SIC liquid mixtures and vapors are then released into the core where they can degrade surrounding fuel rods and interact with the fission products released from fuel. Regarding this last point, iodine fission, product which is a major contributor to the short-to-mid-term

gaseous source term to environment, interacts with the Ag-In-Cd vapors. That significantly affects its speciation and then its transport in the reactor coolant system and in the containment. The thermodynamic study of the ternary Ag-In-Cd phase diagram at high temperature is a necessary step for a reliable estimate of the vaporization of the chemical elements of the absorber material to be able to predict the iodine behavior in case of a severe accident.

Several thermodynamic descriptions of the binary Ag-Cd, Ag-In and Cd-In systems, are available in literature [3-5]. In contrast, for the ternary system at high temperature, the only experimental information available until very recently, was the melting range of the nominal composition of the absorber alloy determined by DSC [2, 6]. Additional measurements have been performed by our team to achieve more accurate description of the system.

Firstly the mixing enthalpy of the liquid phase for five isopleth sections has been measured by silver and cadmium drop dissolution calorimetry at 723 K, and the limits of the biphasic (solid + liquid) domain were derived [7].

Secondly, for three compositions, $Ag_{40}In_{60}$, $Ag_{35}Cd_{05}In_{60}$ and $Ag_{28}Cd_{12}In_{60}$, located in the 60 at.% In isopleth section, the liquidus temperatures have been measured by the so-called Interrupted-Heating Differential Thermal Analysis-IHDTA method [8]. In this thermal analysis protocol, full compositional equilibrium of the sample is approached by the application of interrupted-heating cycles near the expected liquidus temperature.

The aim of this paper is to complete the experimental work and to propose for the first time a thermodynamic modelling of the Ag-Cd-In ternary system. IHDTA is then extended to 9 ternary Ag-Cd-In compositions in order to achieve a more complete description of the liquidus surface (Section 2).

In a first step, a self-consistent set of thermodynamic descriptions of the binaries is required. For this purpose, we have reviewed the available information for the Ag-Cd (Section 4), Ag-In (Section 5) and Cd-In (Section 6) binary systems. The objective is to re-assess the 3 binaries in order to represent the extension of the hcp_A3 phase in the ternary system and to be self-consistent with the current lattice stabilities of the SGTE unary database [10]. The second step is to perform the modeling of the ternary system (Section 7) starting from the combination of the three binary sub-systems. The ternary interaction parameters are optimized based on experimental phase diagram information and calorimetric data for ternary alloys. The optimizations were carried out by taking into account simultaneously all the selected available experimental information, equilibrium phase diagram and thermodynamic properties, with a given weight. The selection of the model parameters and the weights attached to each experimental data were changed by trial and error during the process, until a satisfactory agreement was obtained between the calculated and the experimental data.

2. Experimental

2.1. Materials and Methods

For each composition, silver (Alfa Aesar 99.99%), cadmium (Alfa Aesar 99.9999%) and indium (Alfa Aesar 99.9999%) shots are weighed in stoichiometric proportions. Then, these mixtures of the pure constituents are sealed in silica ampoules under argon with an oxy-acetylene torch. All the sample ampoules are heat treated 1hr at 1273 K before performing

the thermal analyses using a Setaram DSC 111 instrument. The heat flow sensors of this instrument, which can work up to 1103 K, are 3-D thermopiles of high sensitivity. In the experiments, one sample ampoule is inserted into the laboratory tube while an empty silica ampoule of similar weight and shape is inserted in the reference tube. The instrument is temperature-calibrated towards the melting points of Al (Koch light, 99.999%), In (Alfa Aesar, 99.9999%), Sn (Alfa Aesar, 99.9999%) and Zn (Alfa Aesar, 99.999%).

As mentioned in the introduction, the liquidus temperatures are determined using the IHDTA protocol. This method has already been employed for the accurate determination of liquidus temperatures in other systems [11,12]. Principle of the method and its implementation to Ag-Cd-In compositions are described in our previous paper [8].

2.2. Experimental Results

To achieve a better description of the extension of the (liquid + hcp_A3) biphasic region, the liquidus temperatures of 6 new ternary compositions are determined using the IHDTA protocol (**Table 1**). For the sake of completeness, the liquidus temperatures of the three compositions previously studied in the 60 at.% In isopleth section [8] are also reported in **Table 1**.

For the binary composition, our measured value (724-727 K) is in good agreement with the DSC results of Moser et al. [4] (728 K) and Horrocks [6] (729 K).

For the ternary alloys, discrepancies can be seen between the liquidus temperatures measured in this work and those measured by Jones [93] and Robinson [94] by Smith Thermal Analysis. As explained in [8], our thermal analysis protocol is thought to be more reliable and more weight was given to our IHDTA data while modelling the Ag-Cd-In ternary diagram.

Table 1 Liquidus temperatures measured in this and our previous works for various compositions and comparison with literature data. Experimental methods: IHDTA this work and [8], DTA [95], isothermal calorimetry (see text) [7], Smith Thermal Analysis [6, 93-94], DSC [4] and [9].

Alloys composition / at. %			This and our previous works	Literature data
Ag	**Cd**	**In**	**$T_{liquidus}$ / K**	**$T_{liquidus}$ / K**
4.5	23.9	71.6		513, 517 [93] reported in [6]
7.5	23.1	69.4	602±3 [95] 592-595 This work	517 [93] reported in [6]
8	60	32	660-663 This work	
28	60	12	820-823 This work	
15	70	15	746-749 This work	
18	60	22	744-747 This work	
20	20	60	671-674 This work	
37	3	60	-	721 [94] reported in [6]
34	6	60	-	709 [94] reported in [6]
32	8	60	708±3 [95]	
31	9	60		703 [94] reported in [6]
28	12	60	685±3 [95] 676-679 [8]	696 [94] reported in [6]
35	5	60	716±3 [95] 712-715 [8]	
40	0	60	730±3 [95] 724-727 [8]	729 [6] 752 [94] reported in [6] 728 [4] 719.5 [9]
15	30	55	673±3 [95]	
11.0	44.5	44.5	723 [7]	
23.0	15.4	61.6		
30.0	7.0	63.0		

3. Thermodynamic Models

Detailed crystallographic information about the different phases of the ternary system is given in Table 2. As the order-disorder formalism is not supported in the NUCLEA database [96] with which our optimizations will be used, simplified descriptions are chosen for the B2 and $L1_2$ phases.

Table 2 Crystal structure data for the solid phases in the Ag-Cd-In ternary system.

The thermodynamic models of the various phases are briefly introduced below.

The Gibbs energy function ${}^\circ G^\Phi(T) = G^\Phi(T) - H^{SER}$ is referred to the so-called "Standard Element Reference" (SER) state, H^{SER} being the molar enthalpy of the SER state. The temperature dependence of the molar Gibbs energy of the pure elements in either stable or metastable phases, referred to the SER state, is given by the expression:

$$G - H^{SER} = A + BT + CT \ln T + DT^2 + ET^3 + FT^{-1} + GT^7 + HT^{-9}$$

The Gibbs energy functions of the elements are taken from the SGTE (Scientific Group Thermodata Europe) unary database [10]. When not available, metastable structures (necessary as reference values for the thermodynamic description of the corresponding solid solutions) are discussed separately for each phase in the following.

A substitutional model is used for all solution phases, the excess interaction parameters being described by a Redlich-Kister-Muggianu [13, 14] polynomial, and optimized by using the Lukas et al. [1] computer program. The total molar Gibbs energy of the solution phases Φ is expressed under the generic form:

$$G^\Phi = G^{\Phi,ref} + G^{\Phi,id} + G^{\Phi,exbin} + G^{\Phi,exter}$$

In which the reference Gibbs energy is written as:

$$G^{\Phi,ref} = x_{Ag}\ {}^\circ G_{Ag}{}^\Phi + x_{Cd}\ {}^\circ G_{Cd}{}^\Phi + x_{In}\ {}^\circ G_{In}{}^\Phi$$

The ideal mixing contribution as:

$$G^{\Phi,id} = RT\,(x_{Ag} \ln x_{Ag} + x_{Cd} \ln x_{Cd} + x_{In} \ln x_{In})$$

And the binary ($G^{\Phi,exbin}$) and ternary ($G^{\Phi,exter}$) contributions to the excess Gibbs energy as:

$$G^{\Phi,exbin} = x_{Ag}\, x_{Cd} \sum_\nu {}^\nu L^\Phi_{Ag,Cd}\ (x_{Ag} - x_{Cd})^\nu + x_{Ag}\, x_{In} \sum_\nu {}^\nu L^\Phi_{Ag,In}\ (x_{Ag} - x_{In})^\nu + x_{Cd}\, x_{In} \sum_\nu {}^\nu L^\Phi_{Cd,In}\ (x_{Cd} - x_{In})^\nu$$

$$G^{\Phi,exter} = x_{Ag}\, x_{Cd}\, x_{In}\, [x_{Ag}\, {}^{Ag}L^\Phi_{Ag,Cd,In} + x_{Cd}\, {}^{Cd}L^\Phi_{Ag,Cd,In} + x_{In}\, {}^{In}L^\Phi_{Ag,Cd,In}]$$

where ${}^\circ G_i{}^\Phi$ is the molar Gibbs energy of the pure element i in the Φ solution, and x_i the mole fraction of i. The binary ${}^\nu L^\Phi_{i,j}$ and ternary ${}^\nu L^\Phi_{i,j,k}$ interaction parameters can depend linearly on temperature.

The Gibbs energies of the A_pB_q binary stoichiometric compounds are expressed as:

$$G^{ApBq}(T) = a + b\,T + p\,{}^{\circ}G^{ref}_{A} + q\,{}^{\circ}G^{ref}_{B}$$

where the a and b coefficients are respectively the enthalpy $\Delta_f H^{\circ}_{298.15K}$ and entropy $\Delta_f S^{\circ}_{298.15K}$ of formation of the compound. In this model, the heat capacity of a compound is given by the Neumann-Kopp additivity rule, neglecting any possible excess heat capacity. The a and b parameters are to be evaluated during the optimization process. The reference states for pure silver, cadmium and indium are the face-centered cubic (fcc_A1), close-packed hexagonal (hcp_Cd), and tetragonal (tet_A6) structures respectively.

The assessed Gibbs energy parameters are collected in **Table 3**. The PANDAT software is used for plotting most of the figures.

4. Ag-Cd

4.1. Phase Diagram Experimental Information

The Ag-Cd phase diagram has been extensively investigated. By means of thermal and microscopic analyses, the entire liquidus curve and the solidus curves of the α, β and η phases were determined by Rose [28], Bruni and Quercigh [29] and Petrenko and Fedorow [30]. The various liquidus determinations are in rather good agreement.

Later on, Durrant [31] investigated the cadmium-rich part (0-41 at.% Ag) of the phase diagram by thermal and micrographic analyses, and in particular the ε and η solidus lines, and the (ε + η) field boundaries, and completed few years later [32] the ε, γ, β, β' and ζ solid solution boundaries.

Hume-Rothery et al. measured the liquidus in equilibrium with the α solid solution in the 0-39 [33] and 0-16 [34] at.% Cd ranges by thermal analysis on cooling. They also derived the α solidus line and the solubility limit of the α phase in equilibrium with β by micrographic examination of the relative quantities of the 2 phases as a function of temperature.

Using X-ray diffraction, Owen et al. [19] established the boundaries of the stability domains of the solid phases below 973 K. The β'(AgCd) phase is absent from their diagram.

(α + β) field boundaries at 883 K were determined by isopiestic techniques by Rayson and Alexander [35] in disagreement with previous measurements.

From these studies, Hansen and Anderko [25] constructed the phase diagram.

Quader [22] carried out an X-ray investigation to ascertain the phase boundaries at temperatures below 573 K. The presence of the β'(AgCd) phase was confirmed but without establishing its composition domain. The boundaries of the α, ζ and γ phases were in good agreement with those of Owen et al. [19].

Filby and Pratt [37] derived the boundaries of the β phase from activity measurements using a dew point technique.

Horrocks [6] validated all the invariant reactions with Smith Thermal Analysis.

4.2. Thermodynamic Experimental Information

Vapor pressure of cadmium above solid silver-cadmium alloys was measured by several researchers. Above the α phase, isopiestic method was used by Herasymenko [38] in the 873-1173 K temperature range, and by Masson and Sheu [39] at 1063 K, electronic spectrophotometer was used by both Scatchard and Boyd [40] and Rapperport and Pemsler

[41] in the 620-875 and 460-633 K temperature ranges respectively. However, Rapperport et al. did not correctly define the alloy composition and hence their data are not usable.

A dew point technique was used by Birchenall and al. [42] in the 793-1153 K temperature range for 3 α phase compositions, and by Filby and Pratt [37] in the range of temperature 635-1140 K above the α, β, γ and ε phases.

The cadmium activity in the α, β, ζ, γ and ε phases was derived from EMF measurement in the 673-773 K temperature range by Olander [43].

From liquid tin solution calorimetry experiments, various authors derived the heats of formation of the solid phases at different temperatures: Kleppa [44] at 723 K for the α, β, γ and ε phases, Waldman et al. [45] at 273 K and Orr et al. [46] at 308 K for the α phase and Anderson [47] at 304 K for the ζ, β' and γ phases.

Cadmium vapor pressure above the liquid phase was determined by different methods: using a dew point method by Schneider and Schmid [48] in the 973-1123 K temperature and x_{Cd} = 0.266-0.676 composition ranges; by mean of a silica flexible membrane at 1223 K by Van Gool [49]; using an isopiestic method by Conant and Swofford [50] at 773 K for silver rich alloys; using the boiling-point method by Volodin et al. [51] between 823 and 1148 K.

Using EMF measurements, the cadmium activity in the liquid was determined by Schaeffer and Hovorka [52] in the 683-823 K temperature range for cadmium rich compositions, and by Houseman and Conant [53] at 777 K for diluted solutions of silver in cadmium.

Kleppa [44] measured the heat of formation of liquid alloys at 723 K by direct reaction calorimetry.

4.3. Thermodynamic Optimization

A Calphad thermodynamic description of the Ag-Cd binary phase diagram was reported by Horrocks [6] as part of his thesis. First, this optimization is not satisfactory because the domain of non-stoichiometry of the hcp AgCd phase is too narrow whereas an accurate description of this region is of prime importance when considering that this solid solution has a large extension in the ternary. Second, the line separating the ε and (ε + η) domains, in the vicinity of x(Cd) = 0.8, is also not well reproduced. It has been thus decided to completely re-optimize this system.

The three ζ, ε and η solid solutions exhibit the same hcp Mg prototype, but different c/a ratios. In the composition range of the ζ and ε phases, this ratio decreases from about c/a = 1.619 to c/a = 1.555 on increasing cadmium concentration from 47 to 81 at.%. These values are very similar, and close to the ideal 1.63 value corresponding to the close packing of hard spheres. Conversely, the c/a ratio of the η phase (Cd terminal solution) raises from 1.816 to 1.886 on increasing cadmium concentration from 97 to 100 at.%, well above the ideal value. As reported in [6] for Cd, or in [54-56] for Zn, we consider that the dissimilarity in the interatomic spacings creates an energy difference between the lattice stabilities of the ideal and "non-ideal" hcp cadmium forms.

The lattice stability of the hexagonal close-packed cadmium with a "non-ideal" c/a ratio, denoted here hcp_Cd, is taken from the SGTE unary databank [10]. The lattice stabilities of the metastable "ideal" Cd(hcp_A3) and the metastable Cd(bcc_A2) are estimated at the most suitable values during the optimization process, and then fixed.

The AgCd intermetallic phase is modelled as a line compound as it is only stable in a very narrow composition range as shown by [32] who found the 48.7 and 50.3 at.% Cd

compositions to be diphasic between 468 K and 497 K.

The γ-brass structure at high temperature and γ' related superstructure at low temperature have been described as a single Ag_2Cd_3 phase due to the lack of experimental data. Its domain of stability on both sides of the 60 at.% Cd composition (58.6 to 61.8 at.% Cd at T = 300-850 K [19], 57.6 to 61.6 at.% Cd at 773 K [32]) is small justifying to consider this phase as stoichiometric.

The optimization is performed following the guidelines presented in the introduction.

4.4. Results and discussion

The Ag-Cd phase diagram calculated using the optimised set of parameters is compared with the experimental data in **Fig. 1**. Temperatures and compositions of invariant equilibria are compared with experimental values in **Table 4**.

The experimental phase boundaries determined by the different researchers show an overall good concordance. A very good agreement is also observed between calculated and experimental values across the entire system.

Nevertheless, small deviations can be seen in the temperature and compositions of the phase boundaries at the invariant reactions with the γ phase. This results from our choice to model the γ phase as a stoichiometric compound. The ζ/(ζ + γ) lines determined by both Durrant [32] and Owen et al. [19] are not compatible. When the global optimization was carried out, the experimental points from Owen et al. [19] were found easier to reproduce and hence adopted, in the final optimisation.

The calculated ε/(ε + η) line slightly differs from the experimental points because, due to the scarce thermodynamic information on these two phases, we have chosen to restrict the number of optimized interaction parameters.

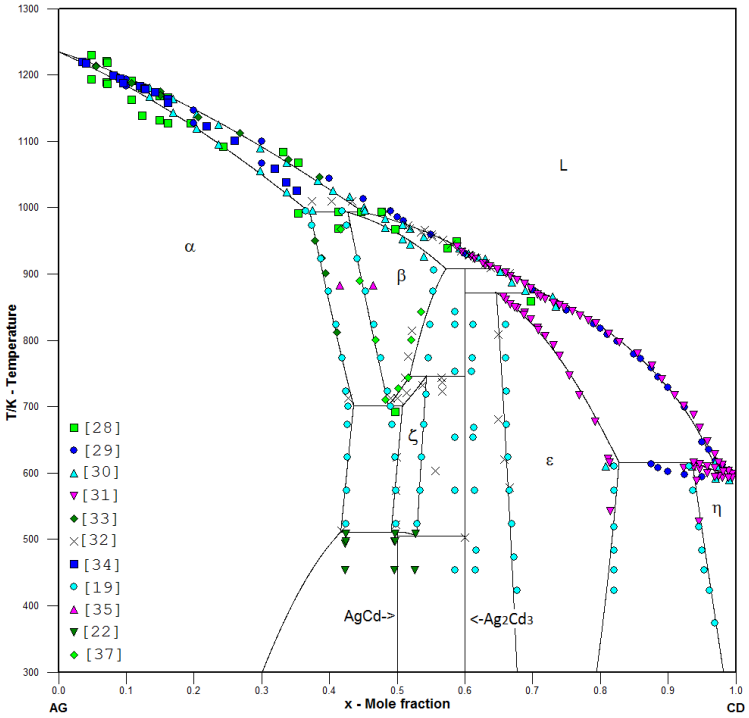

Fig. 1: Ag-Cd calculated phase diagram compared with the experimental points.

Table 3: Gibbs energy functions and interaction parameters of the Ag-Cd-In ternary system.

Table 4: Calculated invariant equilibria in the Ag-Cd, Ag-In and Cd-In systems compared with the literature data.

The calculated formation enthalpy of the liquid phase is compared in **Fig. 2** with the only measured values from Kleppa [44] at high-cadmium content, with a good agreement. For the hcp (ε and ζ) and bcc_A2 (β) phases, the enthalpies calculated with our optimization lie less than 1 kJ/mol above the experimental values obtained by Kleppa [44] and Anderson [47]. This discrepancy is considered acceptable knowing the magnitude of the uncertainty in high temperature solution calorimetry experiments.

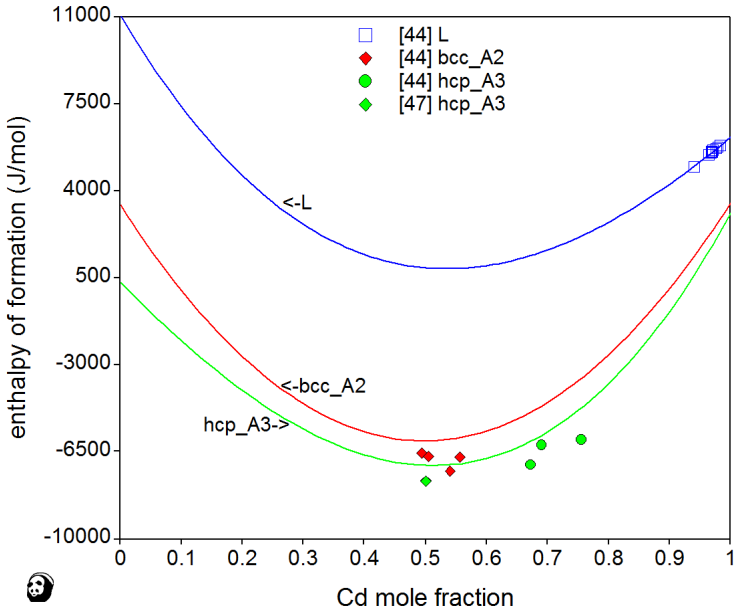

Fig. 2 **Calculated enthalpy of formation of the Ag-Cd liquid, bcc_A2 and hcp phases compared with the experimental values (referred to Ag^{fcc_A1} and Cd^{hcp_Cd}).**

The Cd chemical potential in the liquid phase, calculated at T = 773 K and 1100 K, is plotted vs. Cd mole fraction in Fig. 3 and compared to the experimental data. The highly dispersed experimental values obtained by Volodin et al. [51], those of Schaeffer and Hovorka [52], who themselves judged that their measured activities do not vary in a regular manner with concentration, and few too high values at rich Cd composition discarded by Van Gool [49] himself were not considered in the optimization. The selected data from [48, 50] and [53] are quite well fitted.

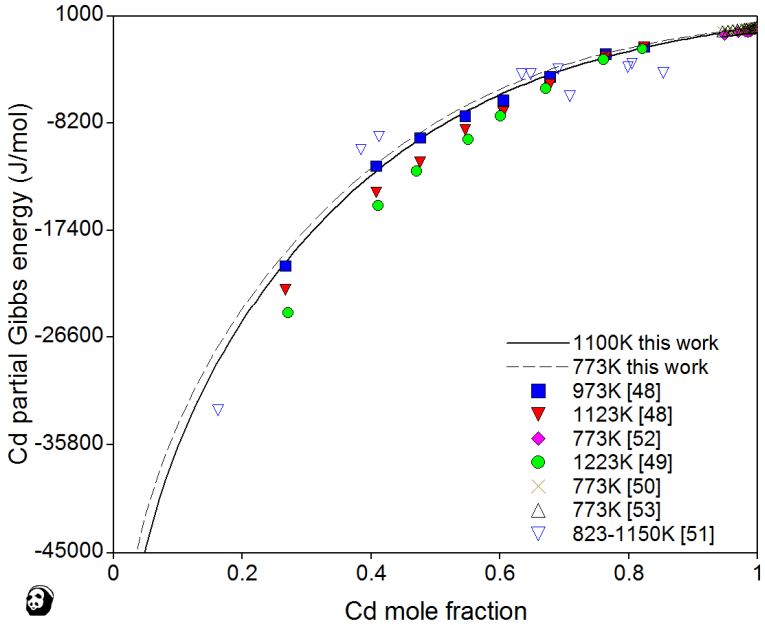

Fig. 3 **Cadmium chemical potential in the liquid phase, referred to Cd^{L}, calculated at T = 773 K and 1100 K, compared with experimental data.**

The calculated formation enthalpy of the α phase (**Fig. 4**) is in agreement with the measured values of Kleppa [44], Waldman et al. [45], and Orr et al. [46]. No variation with temperature could be inferred from these three consistent sets of values.

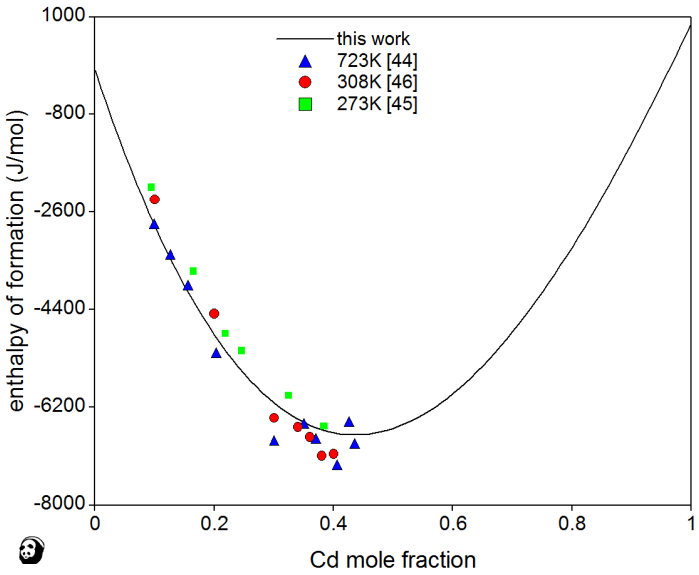

Fig. 4 **Calculated enthalpy of formation of the α phase compared with experimental data, (referred to Ag^{fcc_A1} and Cd^{hcp_Cd}).**

The cadmium chemical potential in the α phase, calculated at T = 700 K and 1000 K is represented in Fig. 5 and compared with all experimental data. A good agreement is

obtained with the data reported by Herasymenko [38], Masson et al. [39] and Birchenall et al. [42]. The calculated curves are less compatible with the values of [37], [40], and [43].

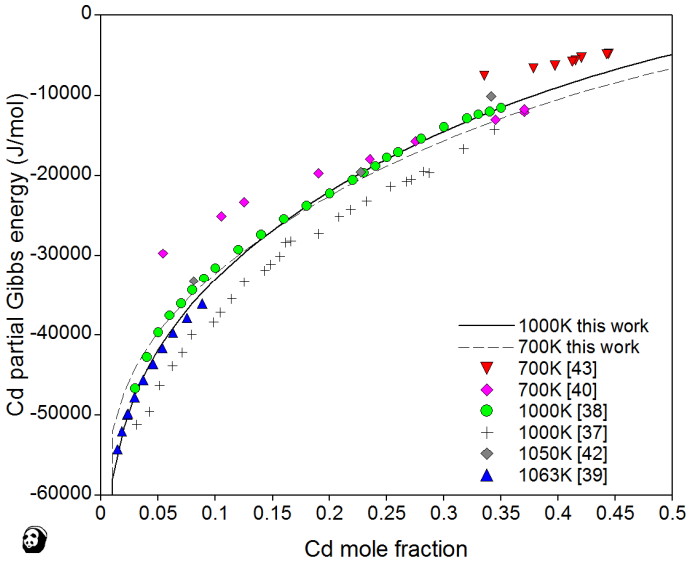

Fig. 5 Cadmium chemical potential in the α phase referred to Cd^L, calculated at T = 700 K and 1000 K, compared with experimental data.

Fig. 6 shows the calculated cadmium partial Gibbs energy in the hcp (ε and ζ) phases and in the bcc_A2 (β) phase, compared with experimental data from Olander [43] and Filby and Pratt [37]. It can be seen that the data series reported by the two authors are in strong disagreement, especially for the ε phase. It was also not possible to correctly reproduce the whole set of a single author. For the hcp phase, values from [43] are in better agreement with the calculation, whereas for the bcc_A2 phase, a mean value between [43] and [37] is calculated.

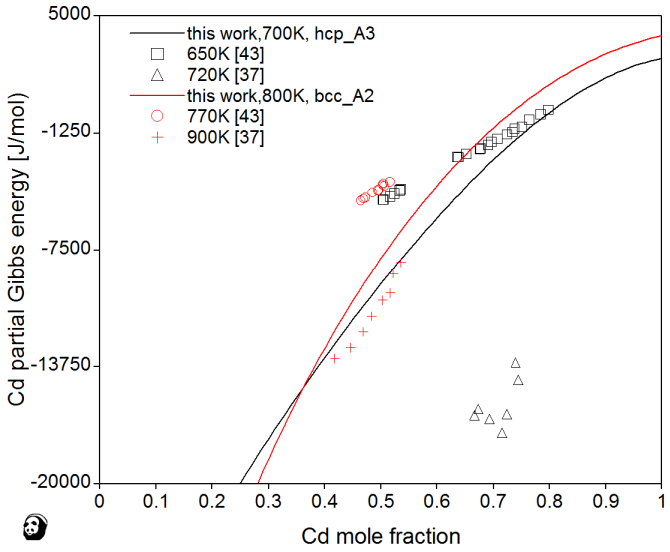

Fig. 6 Cadmium chemical potential in the hcp phase (700 K, black) and in bcc_A2 phase (800 K, red) referred to Cd^L, compared with experimental data.

For the two stoichiometric compounds, the calculated enthalpies of formation match quite well with the available experimental values: $Ag_{0.5}Cd_{0.5}$, $\Delta_f H°_{304K}$ (J/mol) = -9645 this work (-9079 [47]), $\Delta_f H°_{723K}$ (J/mol) = -12716 this work (-9720 [44]); $Ag_{0.4}Cd_{0.6}$, $\Delta_f H°_{304\ K}$ (J/mol) = -7119 this work (-8326 [47]); $\Delta_f H°_{\ 723K}$ (J/mol) = -10804 this work (-10810 [44], -10816 [37]), and are not so far from the DFT calculated value $\Delta_f H°_{0K}$ (J/mol) = -6657 for $Ag_{0.5}Cd_{0.5}$ [58].

5. Ag-In

5.1. Phase Diagram Experimental Information

The phase diagram of the Ag-In system was built by Hansen and Anderko [25] after critical analysis of available experimental investigations. It is essentially based on the results of Weibke and Eggers [59], Hume-Rothery et al. [60-61], Owen and Roberts [62] and Hellner [63]. The more recent works reported thereafter do not significantly modify the phase diagram of [25].

The maximum solubility of indium in α silver has been determined using X-Ray Diffraction (XRD) and metallographic techniques by Straumanis and Riad [64] as x_{In}=0.194 at room temperature, and by Snyder [65] as x_{In} = 0.193 at room temperature and x_{In} = 0.206 at 588 K.

A new phase diagram was constructed by Campbell et al. [66] using differential thermal analysis (DTA), XRD on powder, photomicrography, and Electron Probe Micro-Analysis (EPMA). Compositions ranging from pure indium to 75 at.% Ag were investigated. Above 723 K, the liquidus lies approximately 8 K above the one of Weibke and Eggers [59]. The ζ phase extends to much higher indium concentration than was previously established by [59], and this phase is still stable at room temperature over a very narrow, 70.3 to 71.0 at.% Ag, composition range. The metatectic reaction ζ -> L + Ag_2In was observed at lower temperature.

By means of Smith Thermal Analysis, Horrocks [6] measured the invariants and 2 liquidus points of this system, in very good agreement with previously published works.

Different experimental techniques were used by Moser et al. [4] to investigate the Ag-In phase diagram. By DSC, they determined the temperature of the phase transitions over the whole composition range. Their liquidus temperatures were in agreement with previous studies. With diffusion couples and metallography, they established in particular that the extent of the ζ phase was narrower than previously found by Campbell et al. [66]. The region of stability of the Ag_3In phase was not investigated.

Using DTA, DSC, XRD and EPMA Bahari et al. [67], [9] confirmed the existence of Ag_3In in the composition range between 24.3 and 30 at.% at 298 K.

5.2. Thermodynamic Experimental Information

Concerning the solid phases, the heat of formation was measured by liquid tin solution calorimetry, by Kleppa [44] for the α and ζ solid solutions at 723 K in the x_{In} = 0.078 - 0.535

composition range, and by Orr and Hultgren [68] for the α phase, dropping samples from 317 K in the bath maintained at 700 K, in the x_{In} = 0.05 - 0.17 composition range. In the α phase, both data sets are in excellent agreement.

The activity of indium in the α phase was measured by EMF and gas-solid equilibrium techniques by Alcock and Jacob [69] at 900 K, for compositions ranging from x_{In} = 0.04 to 0.19, and, with an atomic absorption spectrophotometer, by Masson and Pradhan [70] at 1000 K, for compositions ranging from x_{In} = 0.0781 to 0.1817.

There is no information available in literature on the thermodynamic properties of the compounds.

The heat of formation of the liquid phase has been determined by several researchers. The employed technique, the temperature of measurements and the studied composition ranges are compiled thereafter for each study: Kleppa [44], calorimetry, dissolution of solid silver in liquid indium at 723 K, x_{In} = 0.67 - 0.94; Itagaki and Yazawa [71], adiabatic calorimetry at 1243 K, x_{In} = 0.5; Beja [72] and also reported as unpublished work by Castanet et al. [73], direct calorimetry at 1028 K, x_{In} = 0.10 - 0.95; Castanet et al. [73], drop calorimetry at 743 K and 1280 K, x_{In} = 0-1; Sabbar et al. [74], drop calorimetry at 896 K, x_{In} = 0.5.

The activities of silver and indium have been studied combining Knudsen effusion and mass spectrometry by Alcock et al. [75] at 1300 K, for compositions x_{In} = 0.1 - 0.9, and by Qi et al. [76] in the 1100 - 1400 K temperature range and for compositions x_{In} = 0.1 - 0.9.

Using EMF measurements, the activity of indium has been determined by Przezdziedcka - Mycielska et al. [77] at 1000 K and for x_{In} = 0.30 to 0.95, by Nozaki et al. [78] from 1000 to 1200 K and for x_{In} = 0.208 to 0.823, by Kameda et al. [79] in the range of temperature 835 - 1272 K for x_{In} = 0.20 to 0.85, and by Jendrzejczyk and Fitzner [80] between 950 and 1273 K for x_{In} = 0.15 to 1.

Predel and Schallner [81] have measured the activity of zinc in ternary Ag-In-Zn liquid alloys using EMF techniques from which they derived the activity of indium at 1000 K.

5.3. Thermodynamic Optimization

Previous CALPHAD modelling of this system by Chevalier and Fischer [82-84], Korhonen et al. [86] and by Moser et al. [4] are all based on the old lattice stability of In(fcc_A1). Moreover, the Ag_3In phase is omitted in the assessments of Horrocks [6] and Gierlotka [85]. Hence, a new assessment based on the current In(fcc_A1) lattice stability [10] is performed in this study. The very small solubility of Ag in In(tet_A6) is not described. The Ag_2In and $AgIn_2$ phases are considered as stoichiometric compounds due to their narrow phase field. The Ag_3In should rigorously be considered as a non-stoichiometric compound since Bahari [67] established its rather large composition domain of stability extending between 24.3 and 30 at.% In. Nevertheless, considering that this thermodynamic modelling is mainly focused on the high temperature range relevant for nuclear safety assessment under severe accident conditions, the Ag_3In compound, which decomposes above 473 K, is modeled as a stoichiometric compound for the sake of simplicity.

5.4. Results and Discussion

Temperatures and compositions of invariant equilibria are compared with experimental values in **Table 4**. The Ag-In phase diagram calculated using the optimized set of parameters is displayed in **Fig. 7** with the experimental data for comparison.

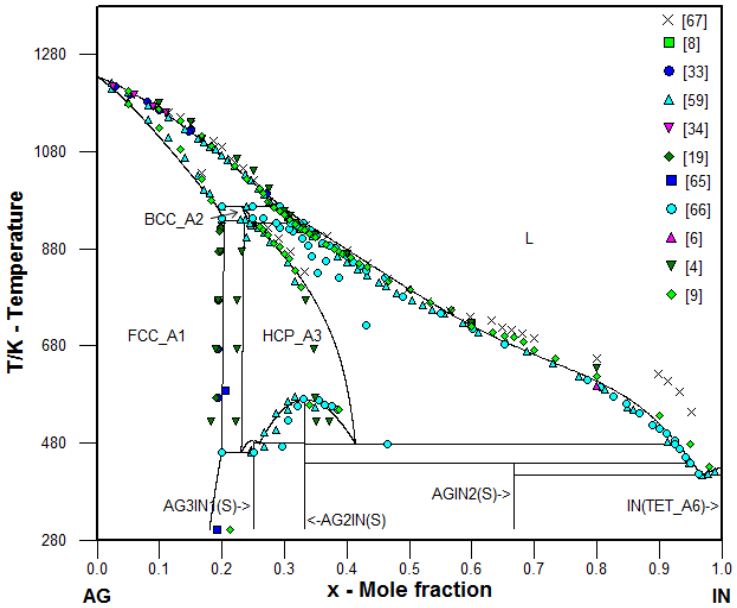

Fig. 7 Ag-In calculated phase diagram compared with experimental points.

It can be seen that, excepting [67], there is an overall good agreement between the liquidus temperatures measured by the different authors. Significant discrepancies with the results of Bahari [67] are observed in the indium-rich region. According to our experience on this system, a possible explanation could be the sluggish diffusion in the hcp_A3 solid solution in equilibrium with the liquid making the liquidus detection by DSC uncertain, particularly in the In-rich region where the liquidus temperatures are low. It must be stressed that the liquidus temperatures measured later by the same authors [9] are in better agreement even if they are still somewhat above the other values. The experimental values are relatively well reproduced by the assessment. Nevertheless, the calculated liquidus is slightly higher than most of the experimental values in the 750-850 K area, and similar disagreements are observed in this range for the optimizations of [6], [4], [85]. When trying to better reproduce this range, the calculated liquidus is then lowered between 500 and 750 K and the agreement with the experimental points is degraded in this last range, this is the case with the assessment from [86].

The extent of the hcp field according to the consistent works of Weibke and Eggers [59] and Moser et al. [4] contradicts the results of Campbell et al. [66]. The narrower extent of the hcp domain at high temperature reported by [59] was found to be compatible with the thermodynamic description, and thus selected for the new assessment. According to Campbell et al. [66], the (Ag_2In + hcp) domain would be asymmetrical but this shape is judged unlikely by [87]. The optimization based on the experimental points from Weibke and Eggers [59] for the (Ag_2In + hcp) silver rich domain leads to a symmetric shape, the hcp composition reaches 42 at.% In at the metatectic temperature of 477 K. In the calculated

phase diagram, the hcp solid solution is not stable at room temperature and decomposes by the eutectoid reaction hcp → fcc_A1 + Ag_3In.

The boundaries of the (fcc_a1 + hcp) diphasic domain determined by Moser et al. [4] have been discarded along with their other points, which seem always shifted relative to the other works. For this domain, the value of the solubility of indium in fcc_A1 is calculated in better agreement with the data measured by [64-66], than with those from [60] and [62]. However, further investigations are needed to clarify the solid phase equilibria in the 20 - 50 at.% In range at low temperature.

The calculated enthalpy of formation of the liquid phase is compared in **Fig. 8** with the experimental values. No clear temperature dependence of the mixing enthalpy arises from the experimental data.

The silver and indium chemical potentials, calculated at T = 1000 K and 1300 K in the liquid are shown in **Fig. 9.** A good agreement is observed with most of the experimental data, excepting those of Nozaki et al. [78], which are higher than all other measured values, and those of Predel et al. [81], obtained by extrapolation of Ag-In-Zn ternary data and which are lower. These two sets of data have not been taken into account in the optimization.

The enthalpy of formation calculated for the α phase at 723 K is in close agreement with the experimental data, whereas for the ζ phase, the calculated values are slightly less exothermic than the experimental data obtained by Kleppa [44] and Orr and Hultgren [68] (**Fig. 10**).

The In chemical potential in the α phase calculated at T = 950 K is reported in **Fig. 11**. The experimental data from Alcock et al. [69] and Masson and Pradhan [70] are quite well fitted.

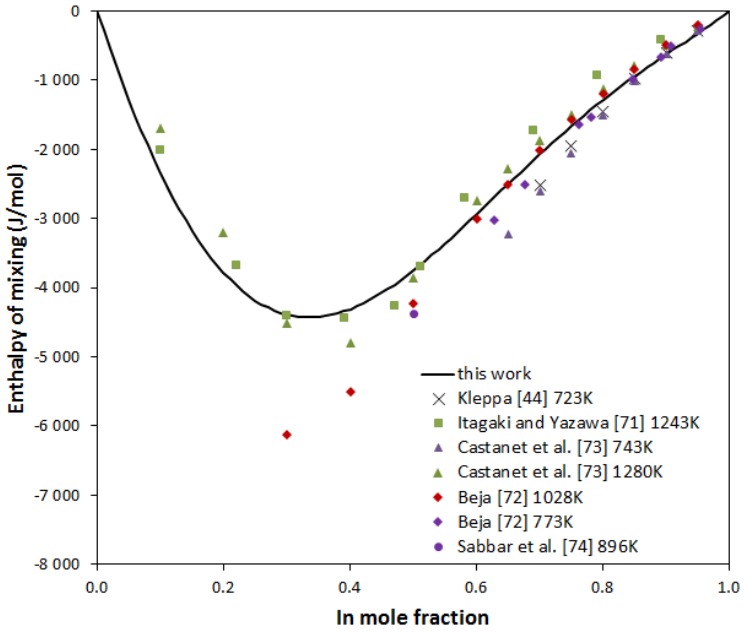

Fig. 8 **Calculated enthalpy of formation in the liquid phase compared with the experimental values (referred to liquid).**

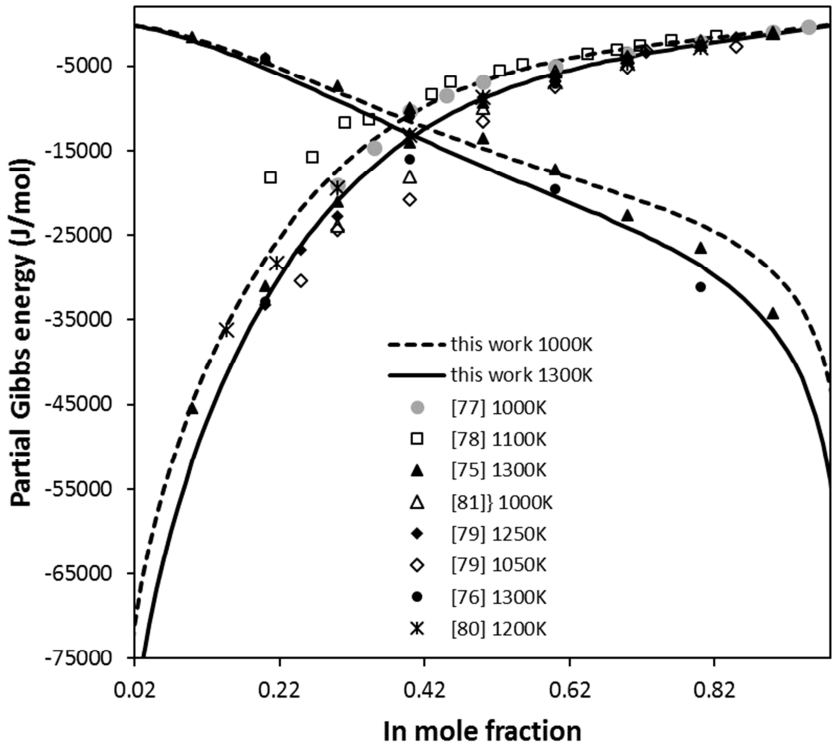

Fig. 9 **Ag and In chemical potentials in the liquid calculated at T = 1000 K and 1300 K compared with the experimental values (referred to liquid).**

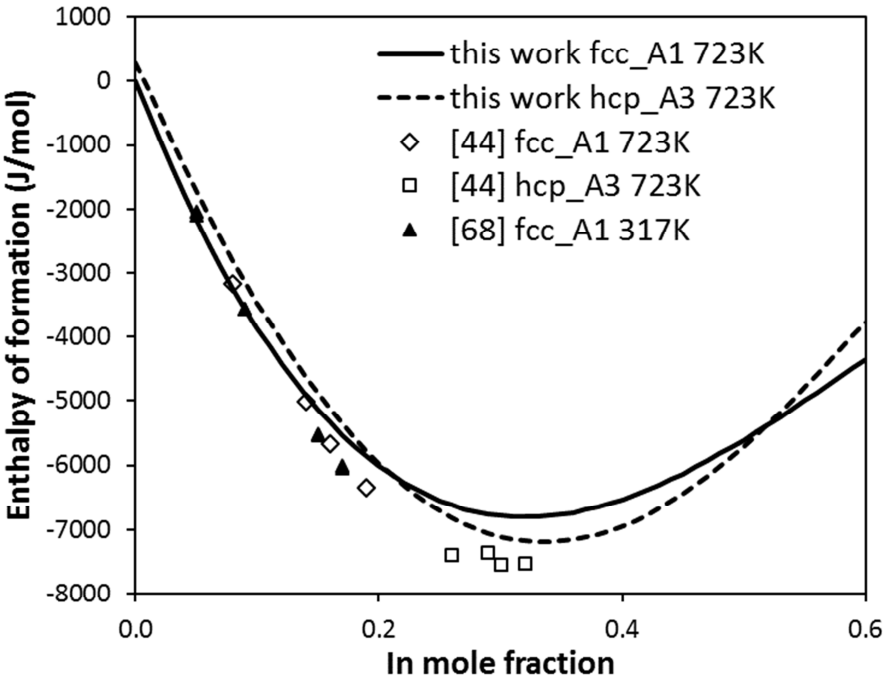

Fig. 10 Calculated enthalpy of formation in the α and ζ phases at 723 K compared with experimental data (referred to Ag^{fcc_A1} and In^{L}).

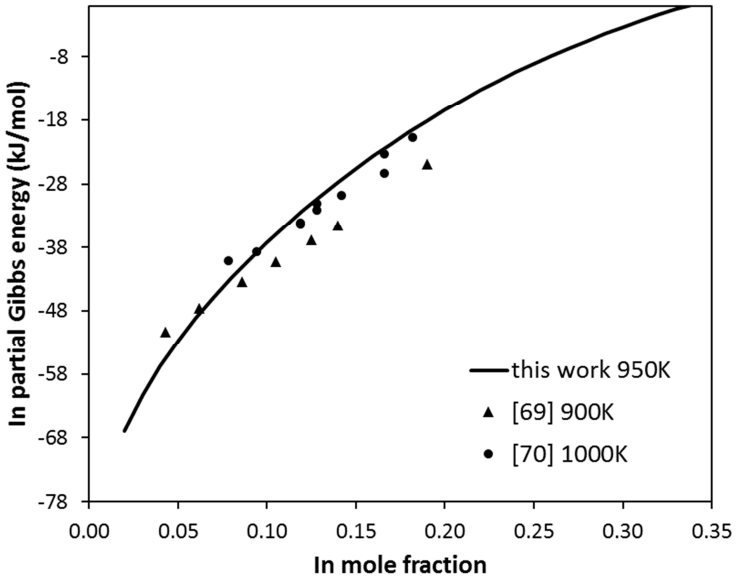

Fig. 11 Indium chemical potential in the α phase referred to the liquid phase, calculated at T = 950 K and compared with experimental data.

The Gibbs energies of the compounds have been entirely estimated by the optimization. The calculated enthalpies of formation can be compared with DFT calculations at 0 K: $Ag_{0.75}In_{0.25}$, $\Delta_f H°_{298K}$ (J/mol) = -6574 this work, -5384 [88], -4728 [58], $Ag_{0.666}In_{0.333}$, $\Delta_f H°_{298K}$ (J/mol) = -7892 this work, -4699 [88], -4536 [58], $Ag_{0.333}In_{0.666}$, $\Delta_f H°_{298K}$ (J/mol) = -4166 this work, -4014 [88], -3859 [58]. The order of magnitude is consistent for $Ag_{0.75}In_{0.25}$ and $Ag_{0.333}In_{0.666}$. Contrariwise, for the composition $Ag_{0.666}In_{0.333}$, the DFT calculations do not predict a stable compound. The thermodynamic description could be improved with additional experimental thermodynamic properties for the three compounds.

6. Cd-In

A Calphad assessment of the Cd-In system has been published by Dutkiewicz et al. [5]. It is based on the old lattice stability for the unary In(fcc_A1) [10]. To achieve compatibility with our new Ag-In binary description, the interaction parameters for the fcc_A1 and tet_A6 phases are re-evaluated here. The calculated phase diagram is presented in Fig. 12 and the invariant temperatures compared in Table 4. The fcc_A1 phase field cannot be correctly fitted with the new lattice. It is not expected that this discrepancy, which occurs around room temperature, can significantly affect the calculations at high temperatures.

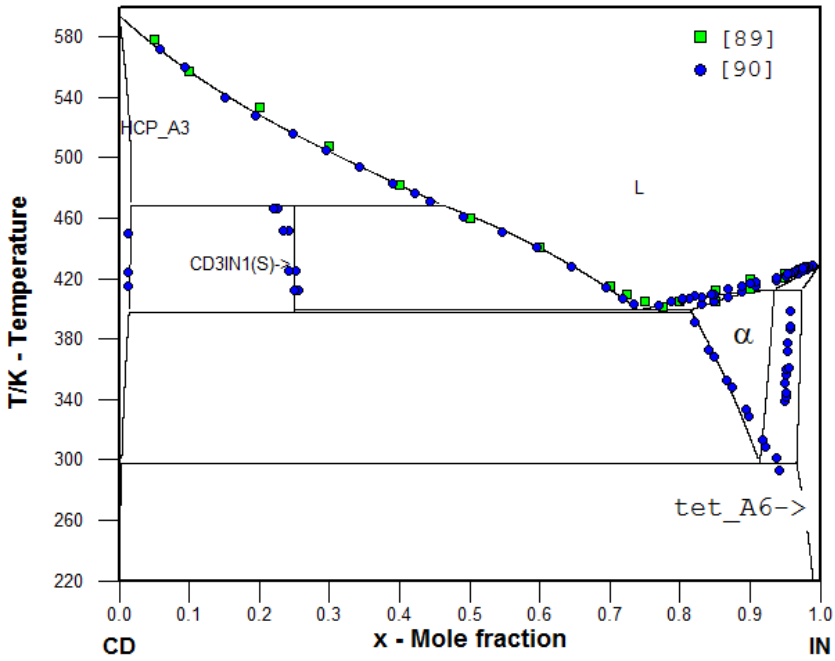

Fig. 12 **Cd-In phase diagram recalculated from the optimized parameters, compared to the experimental points from Heumann and Predel [89], and Rosina [90].**

7. Ag-Cd-In

7.1. Experimental Information

The fcc_A1(Ag)/(fcc_A1(Ag) + hcp_A3) line was established by Snyder [65] combining XRD and metallographic techniques at room temperature and at 588 K.

Horrocks [6] determined the liquidus at 1098.5 K by differential scanning calorimetry for an alloy of control rod composition 80Ag-5Cd-15In wt.%, which is in complete agreement with other literature values 1095 ± 25 K [91], 1100 ± 10 K [92], 1104 K [2]. He reported liquidus arrest temperatures of ternary silver alloys measured by Jones [93] between 513 and 517 K in the Cd/In = 1/3 section, and by Robinson [94] between 696 and 721 K in the x_{In} = 0.6 section. The solidus for the control rod composition is given at 998 K [6] and at 1016 K [2].

The enthalpy of mixing in Ag-Cd-In liquid alloys along five isopleth sections corresponding to the ratios Cd/In = 1/1, Cd/In = 1/4, Cd/In = 1/9 and Ag/In = 1/4, Ag/In = 1/19 was measured by Benigni et al. [7] using drop calorimetry at 723 K. The liquidus line at this temperature was tentatively drawn from the slope changes on the partial mixing enthalpy curves (Table 1). The liquidus was also investigated by conventional DTA/DSC and the solvus compositions were also determined by optical micrograph and scanning electron microscopy on equilibrated and quenched samples by Decreton [95]. His values are reported in Table 1 in comparison with this work and the liquidus temperatures reported in [8]. The main objective of the additional experimental work reported in this paper (Table 1) was to

complete the previous work by investigating the Cd-rich part of the ternary diagram poorly investigated up to now.

7.2. Optimization and discussion

Horrocks [6] calculated the Ag-Cd-In system by only combining the three optimized binary descriptions. Desgranges [96] reported a ternary isothermal section calculated at 623 K from a Calphad modelling. Ternary excess Gibbs energy parameters are added in the fcc_A1 and hcp_A3 phases to represent the continuous biphasic (fcc_A1 + hcp_A3) phase field extending from the Ag-Cd to the Ag-In binary borders, which does not exist in Horrocks's sections.

In this work, at first, excess ternary parameters were optimized for the liquid and hcp_A3 phases, based on the experimental data from [95], [7], [8] and this work. For the liquidus temperatures, a high weight was given to the data from the two latter experimental investigations relying on the IHDTA protocol. In this protocol, as discussed in detail in [8], conditions much closer to equilibrium are approached, reducing the uncertainty of the liquidus temperature measurements.

Then, these parameters were fixed, and for the fcc_A1 phase, which is present in the Ag-rich area on the one hand, and in the In rich area on the other hand, positive ternary interaction terms are evaluated to counteract a high solubility of Cd in the Ag rich phase, in order to well reproduce both the extents of the fcc_A1 and (fcc_A1 + hcp_A3) domains in accordance with Snyder [65] results at 300 K and 588 K, and the liquidus and solidus temperature at the SIC composition.

The excess ternary interaction parameters are reported in **Table 3**. The calculated and measured integral and partial enthalpies of mixing in the liquid are compared in **Fig.13 a-j**. The agreement is fair for the integral enthalpy values. Regarding the Ag partial values for Cd/In = 1/4 (fig. 13d) and Cd/In = 1/9 (fig. 13f) and for $x_{Ag} > 0.2$, the discrepancy could be due to several reasons. Firstly, a fraction of the difference between the fit and the experimental data can be explained by the uncertainty on the measurement of the silver partial enthalpy, estimated to be around 0.5 $kJ.mol^{-1}$ [7]. Secondly, from a general point of view, silver dissolution in Ag-Cd-In liquid is a rather slow process. Kleppa [44] already highlighted this point in reporting his experiments of solid silver dissolution in liquid cadmium. Moreover, as the solubility limit is approached by successive additions of silver samples, the driving force for Ag dissolution gradually decreases and the kinetics slows down. It is hence possible that dissolution of the last samples could be incomplete.

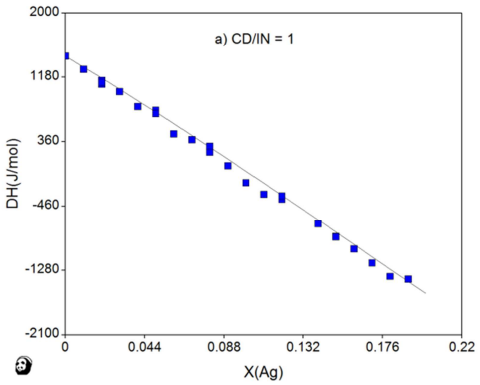
a) CD/IN = 1
DH(J/mol)
2000
1180
360
-460
-1280
-2100
0
0.044
0.088
0.132
0.176
0.22
X(Ag)

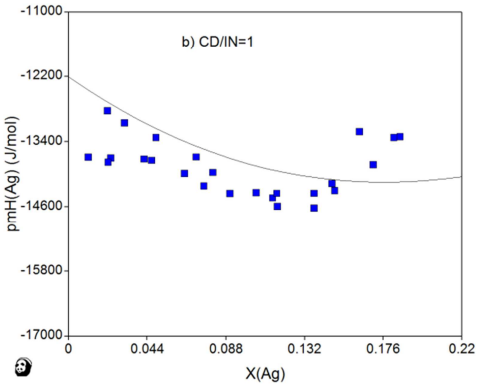
b) CD/IN=1
pmH(Ag) (J/mol)
-11000
-12200
-13400
-14600
-15800
-17000
0
0.044
0.088
0.132
0.176
0.22
X(Ag)

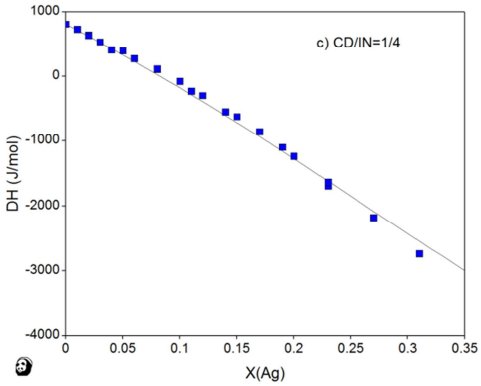
c) CD/IN=1/4
DH (J/mol)
1000
0
-1000
-2000
-3000
-4000
0
0.05
0.1
0.15
0.2
0.25
0.3
0.35
X(Ag)

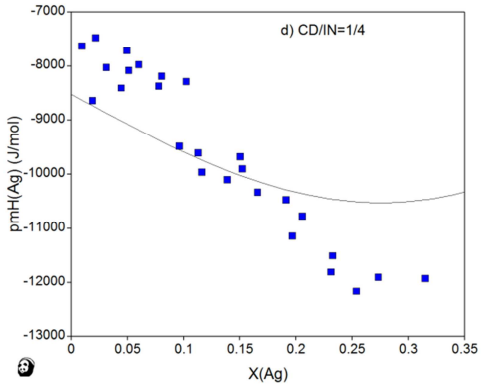
d) CD/IN=1/4
pmH(Ag) (J/mol)
-7000
-8000
-9000
-10000
-11000
-12000
-13000
0
0.05
0.1
0.15
0.2
0.25
0.3
0.35
X(Ag)

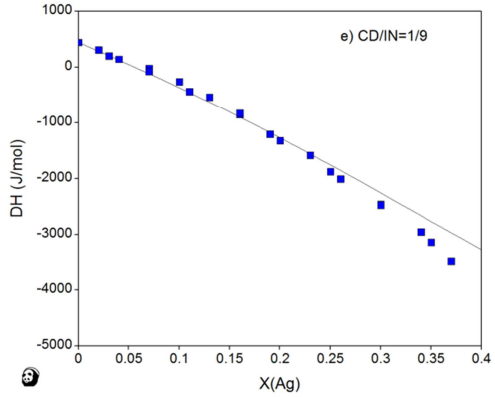
e) CD/IN=1/9
DH (J/mol)
1000
0
-1000
-2000
-3000
-4000
-5000
0
0.05
0.1
0.15
0.2
0.25
0.3
0.35
0.4
X(Ag)

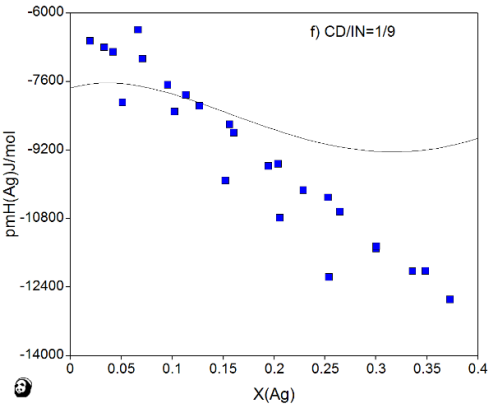
f) CD/IN=1/9
pmH(Ag)J/mol
-6000
-7600
-9200
-10800
-12400
-14000
0
0.05
0.1
0.15
0.2
0.25
0.3
0.35
0.4
X(Ag)

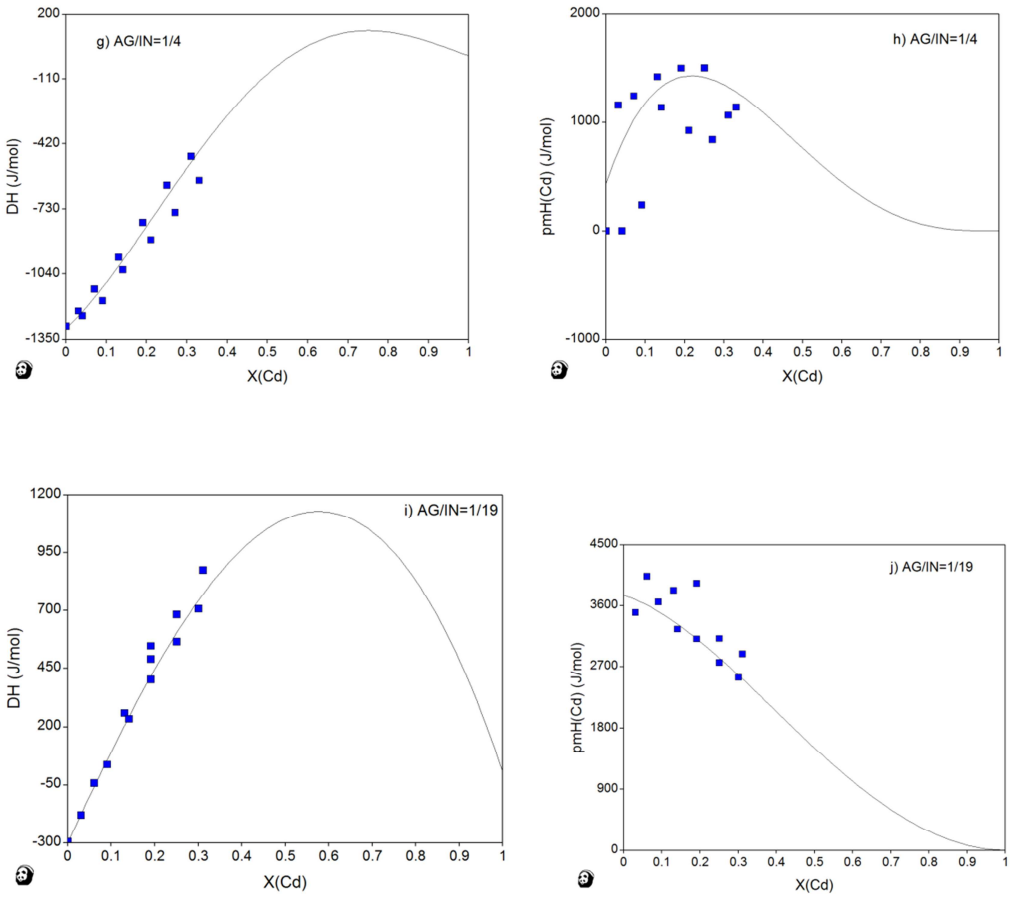

Fig. 13 a-j Calculated integral and partial enthalpy of mixing in the liquid phase, compared to the experimental data from Benigni et al. [7].

Calculated isopleth sections at Cd/In=1/3, x_{In} = 60 at.%, and x_{Cd} = 60 at.% compared to experimental data, and isothermal sections at 821 K, 746 K, 723 K, 673 K, and 593 K are presented in Fig. 14 a-c, and Fig 15 a-e respectively, showing a good agreement with the experimental data. The calculated isothermal section at 723 K (Fig. 15 c), optimized by taking into account the more recent liquidus temperature determination reported in this paper and in [8], exhibits a significant discrepancy with our previous results [7] and [95]. In our experimental study of the system, we have tried to gradually improve the accuracy of the liquidus temperature determinations, starting firstly by a rather indirect approach based on the examination of the partial enthalpy curves [7], secondly by classical DTA/DSC [95], for which we put in evidence some limitations in this ternary system [8] and finally by IHDTA.

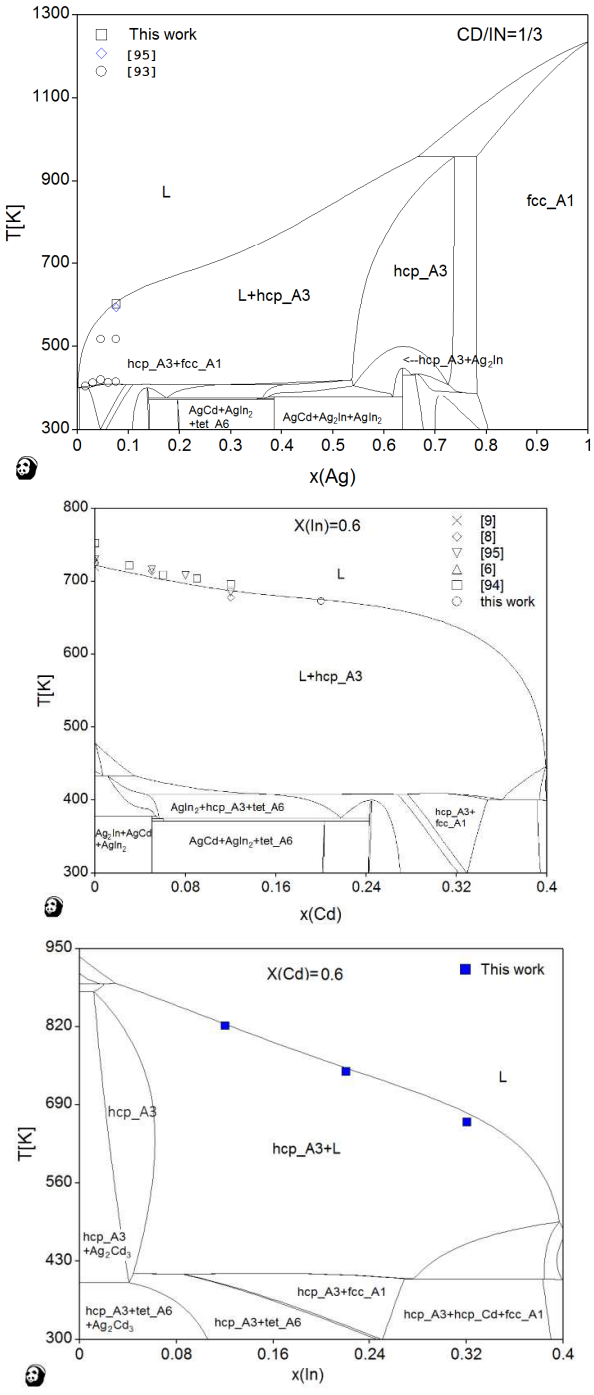

Fig. 14 a-c Calculated isopleth sections at Cd/In=1/3, x_{In} = 60 at.%, and x_{Cd} = 60 at.%, compared to the experimental data.

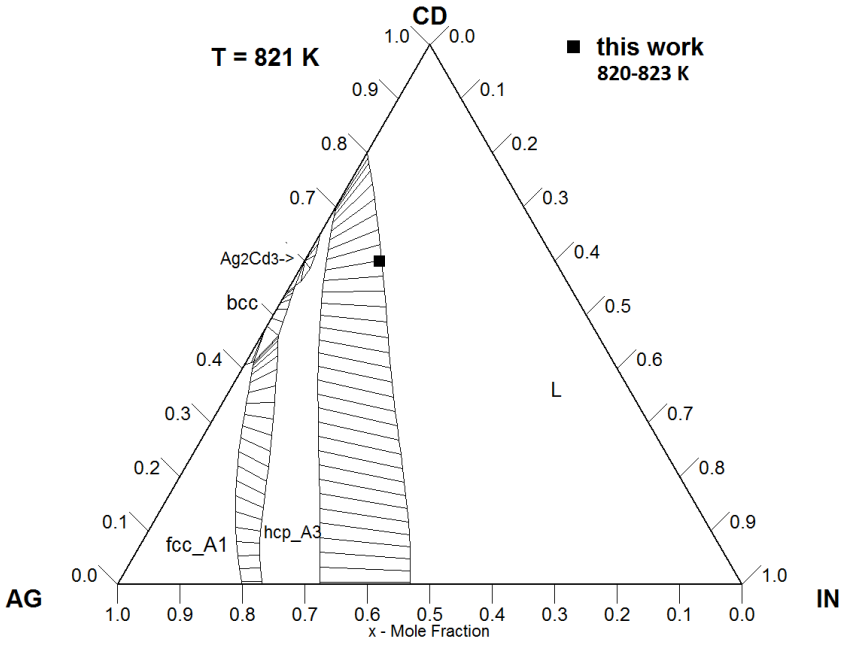
CD
T = 821 K
this work
820-823 K
Ag2Cd3->
bcc
L
fcc_A1
hcp_A3
AG
IN
x - Mole Fraction

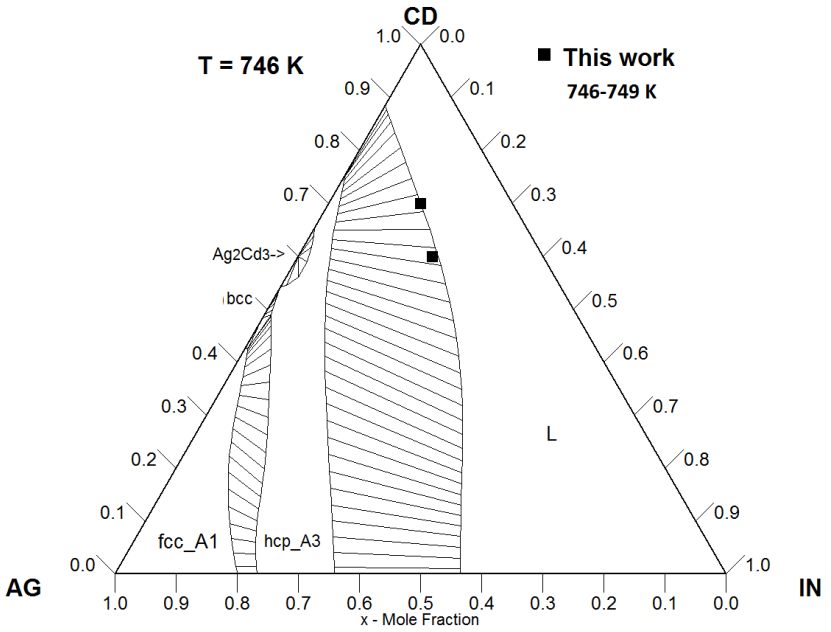
CD
T = 746 K
This work
746-749 K
Ag2Cd3->
bcc
L
fcc_A1
hcp_A3
AG
IN
x - Mole Fraction

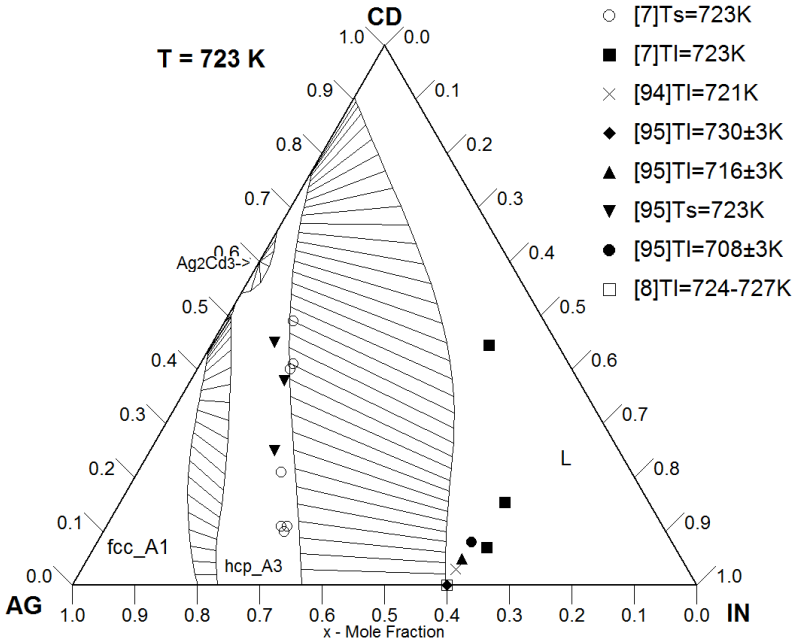
T = 723 K
CD
AG
IN
x - Mole Fraction
Ag2Cd3->
fcc_A1
hcp_A3
L
[7]Ts=723K
[7]Tl=723K
[94]Tl=721K
[95]Tl=730±3K
[95]Tl=716±3K
[95]Ts=723K
[95]Tl=708±3K
[8]Tl=724-727K

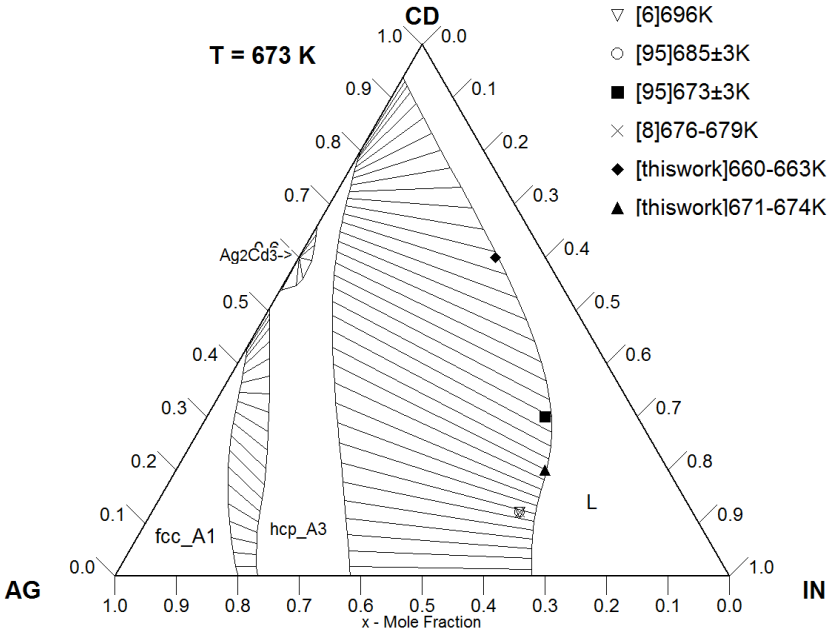
T = 673 K
CD
AG
IN
x - Mole Fraction
Ag2Cd3->
fcc_A1
hcp_A3
L
[6]696K
[95]685±3K
[95]673±3K
[8]676-679K
[thiswork]660-663K
[thiswork]671-674K

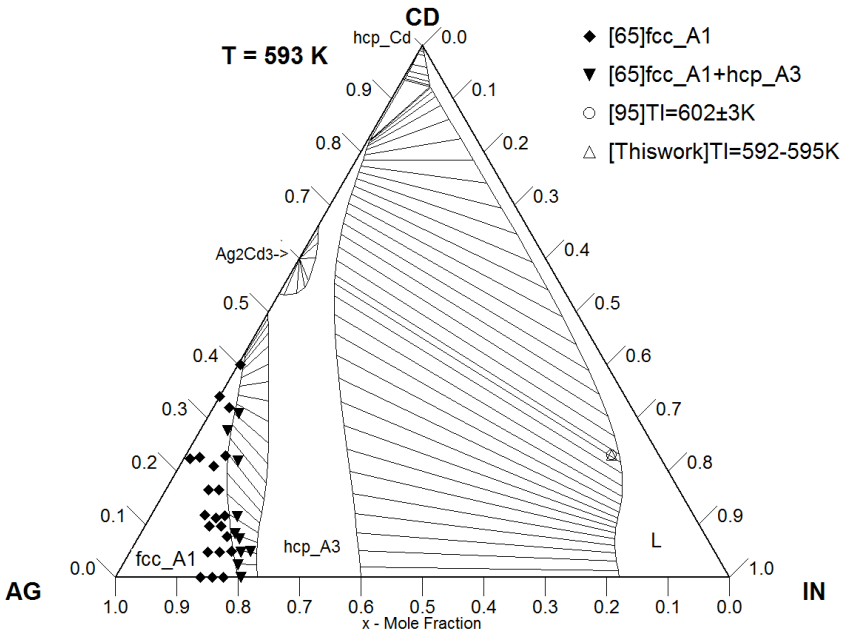

Fig. 15 a-e Isothermal sections calculated at 821, 746, 723, 673 and 593 K, compared to the experimental data.

The boundary between the monophasic fcc_A1 and biphasic (fcc_A1 + hcp_A3) domains at 588 K from Snyder [65] is well reproduced (Fig. 15e). At room temperature, the extent of the hcp_A3 phase field by [65] is questionable, because the AgCd and Ag_3In compounds are known to be stable in the binary systems at this temperature.

With the global description, the temperature of fusion of the control rod alloys of nominal composition is calculated at 1099 K, compared to 1095 ± 25 K [91], 1100 ± 10 K [92], 1098.5 K [6], 1104 K [2], and the solidus temperature is calculated at T = 1002 K, compared to 998 K [6] and 1016 K [2].

8. Conclusion

The thermodynamic assessment of the Ag-Cd-In ternary system based on the exhaustive compilation of literature data and recent experimental investigations [95] [7], [8] has been carried out. It also takes into account new experimental data related to the liquidus temperatures in cadmium-rich region which are reported in this paper. The liquidus temperatures for ternary compositions have been determined by using the IHDTA protocol. It has been shown in [8] that this method, operating closer to equilibrium conditions, considerably reduces the uncertainty in the liquidus determination for this system.

The obtained dataset of thermodynamic parameters allows a general good agreement between experimental and calculated results on the binary Ag-In, Ag-Cd and In-Cd subsystems and on the ternary system, at high temperature, in compositions domains where liquid phase is present. It is required to add ternary interaction parameters in the excess Gibbs energy expressions of the solution phases to fit the mixing enthalpy of the liquid and the extents of the (hcp_A3 + liquid) and (fcc_A1 + liquid) biphasic domains which have been experimentally determined. Additional experimental investigations such as thermodynamic

data of the solid phases could be of high interest to increase the accuracy of the ternary excess interaction parameters of the hcp_A3 and fcc_A1 solid solutions.

Acknowledgements: The authors wish to thank the GDR CNRS No.3584 TherMatHT where fruitful discussions started and led to collaborations on the present project.

[1] H.L. Lukas, E.Th. Henig and B. Zimmermann, Optimization of Phase Diagrams by a Least Squares Method using Simultaneously Different Types of Data, CALPHAD, 1977, 1(3), p 225-236.
[2] M. Steinbrück, U. Stegmaier, Experiments on Silver-Indium-Cadmium Control Rod Failure During Severe Accidents Sequences, Jahrestagung Kerntechnik 2010, annual meeting on nuclear technology, 4-6 mai 2010, *bcc Berliner Congress Center.,* M. Steinbruck, U. Stegmaier, U. and M. Grosse, Experiments on Silver-Indium-Cadmium Control Rod Failure During Severe Nuclear Accidents, Ann. Nucl. Energy 101 (2017) p 347-358.
[3] P. Y. Chevalier and E. Fischer (2004), unpublished assessment supplied to SGTE and included in the SGTE database solution v4.1 (january 2005), and included in Landolt-Bornstein, Thermodynamic Properties of Inorganic Materials, Group IVB, 19(5), Springer-Verlag Berlin Heidelberg, (2007).
[4] Z. Moser, W. Gasior, J. Pstrus, W. Zakulski, I. Ohnuma, X.J. Liu, Y. Inohana and K. Ishida, J. Electron. Mater., 30(9) (2001) p 1120-1128.
[5] J. Dutkiewicz, L. Zabdyr, W. Zalulski, Z. Moser, J. Salawa, P.J. Horrocks, et al., Cd-In (Cadmium-Indium), J. Phase Equilibria 13 (1992) p 261-269.
[6] P.J. Horrocks, Phase Diagram and Thermodynamics of the Ag-Cd-In Ternary Alloys Systems, Ph D. thesis, Manchester University (1991).
[7] P. Benigni, S. Hassam, A. Decreton, G. Mikaelian, K. Gajavalli, M. Barrachin, E. Fischer and J. Rogez, Enthalpy of Mixing in the Ag-Cd-In Ternary Liquid Phase, Journal of Chem. Thermodynamics, 107 (2017) p 207-215.
[8] K. Gajavalli, G. Mikaelian, M. Barrachin, A. Decreton, E. Fischer, J. Rogez and P. Benigni, Journal of Thermal Analysis and Calorimetry, doi.org/10.1007/s10973-018-7442-1 (2018).
[9] Z. Bahari, M. Elgadi, J. Rivet and J. Dugué, Experimental Study of the Ternary Ag–Cu–In Phase Diagram, J. Alloys Compd. 477 (2009) p 152–165.
[10] PURE 5.0 SGTE Pure Elements (Unary) Database, Scientific Group Thermodata Europe 2009.
[11] K.-W. Moon, W.J. Boettinger, U.R. Kattner, F.S. Biancaniello and C.A. Handwerker, Experimental and Thermodynamic Assessment of Sn-Ag-Cu Solder Alloys, J. Electron. Mater., 29 (2000) p 1122-1136.
[12] R.J. Wu and J.H. Perepezko, Liquidus Temperature Determination in Multicomponent Alloys by Thermal Analysis, Metall. Mater. Trans. A 31(2000) p 497-501.
[13] O. Redlich and A.T. Kister, Optimization of Phase Diagrams by a Least Square Method Using Simultaneously Different Types of Data, Ind. Eng. Chem. 40(2) (1948) p 345-348.
[14] Y.M. Muggianu, M. Gambino and J.P. Bros, Enthalpy of Formation of Liquid Bi-Sn-Ga Alloys at 723 K. Choice of an Analytical Expression of Integral and Partial Excess Quantities of Mixing, J. Chim. Phys. Phys.-Chim. Biol. 72(1) (1975) p 83-88.
[15] Von H. Astrand and A. Westgren, Rontgenanalyse der Silber-Cadmiumlegierungen, Z. Anorg. Chem. 175 (1928) p 90-96.
[16] G. Natta and M. Freri, Analisi Coi Raggi X e Structtura Cristallina Delle Leghe Cadmio-Argento, Atti Reale Acad. Dei Lincei Rendiconti 6 (1927) p 422-428, p 505-511; 7 (1928) p 406-410.
[17] V.M. Goldschmidt, Z. Physik. Chem., 133 (1928) 397-419.
[18] A. Wolf, Transformations in the Solid State in Silver-Cadmium Alloys, Z. Anorg. Chem. 189 (1930) p 152; Z. Metallkd. 14 (1932) p 270; Z. Metallkd. 22 (1930) p 369.
[19] E.A. Owen, J. Rogers and J.C. Guthrie, An X-Ray Study of Silver-Cadmium Alloys, J.

Inst. Met. 65 (1939) p 457-472.
[20] K. Moeller, X-ray Examination of the Sections Ag5Sn-AgCd2 and Ag5Sn-AgCd in the System Ag-Cd-Sn, Z. Metallkd 34(1942) p 171-172, (1942).
[21] L. Muldawer, M. Amsterdam and F. Rothwarf, The Silver-Cadmium Beta and Zeta Phases, Trans. AIME 197 (1953) p 1458-1459.
[22] M.D.A. Quader, An X-Ray Study of Silver-Cadmium Alloys, Indian J. Phys. 34 (1960) p 506-515.
[23] M.D.A. Quader and B.N. Dey, Lattice Expansion and Debye temperature of α-phase Ag-Cd alloy, Indian J. Phys. 36 (1962) p 43-54.
[24] B. Henderson and G.V. Raynor, Lattice Spacings in the Binary Silver-Cadmium System, J. Inst. Met 90 (1961-1962) p 484-486.
[25] M. Hansen and K. Anderko, Constitution of Binary Alloys, Mc-Graw-Hill Book Company, New-York, Toronto, London, 1958.
[26] R.P. Elliott, Ph.D., “Constitution of Binary Alloys”, First Supplement, Mc-Graw-Hill Book Company, New-York, St Louis, San Fransisco, Toronto, London, Sydney, (1965).
[27] P. Villars, K. Cenzual, Pearson's Crystal Data - Crystal Structure Database for Inorganic Compounds, Release 2015/16, ASM International, Materials Park, Ohio, USA
[28] T.K. Rose, On Certain Properties of the Alloys of Silver and Cadmium, Proc. Roy. Soc. (London) 74 (1905) p 218-230.
[29] G. Bruni and E. Quercigh, Uber das Zustandsdiagramm der Silber Cadmium Legierungen, Z. Anorg. Chem. 68 (1911) p 198-206.
[30] G.J. Petrenko and A.S. Fedorow, Uber die Leguerungen des Silbers mit Cadmium, Z. Anorg. Chem. 70 (1911) p 157-168.
[31] P.J. Durrant, The Constitution of the Cadmium-Rich Alloys of the System Cadmium-Silver, J. Inst. Met. 45 (1931) p 99-118.
[32] P.J. Durrant, The ε, γ, and β phases of the System Cadmium-Silver, J. Inst. Met. 56 (1935) p 155-164.
[33] W. Hume-Rothery, G.W. Mabbott and K.M.C. Evans, The Freezing-points, Melting Points, and Solid Solubility Limits of the Alloys of Silver and Copper with the Elements of the B Sub-Groups, Philos. Trans. 233 (1934) p 1-97.
[34] W. Hume-Rothery and P.W. Reynolds, The Accurate Determination of the Freezing-points of Alloys, and a Study of Valency Effects in Certain Alloys of Silver, Proc. Roy. Soc. (London) A160 (1937) p 282-303.
[35] H.W. Rayson and W.A. Alexander, Isopiestic Techniques Applied to Phase-Diagram Determination in the Systems Silver-Cadmium and Copper-Cadmium, Can. J. Chem. 35 (1957) p 1571-1575.
[36] W.G. Moffatt, The Handbook of Binary Phase Diagrams, Genium Publication Corp. (updated 02/1998).
[37] J.D. Filby and J.N. Pratt, A Vapour Pressure Study of the Thermodynamic Properties of the Alpha, Beta, Gamma and Epsilon Silver-Cadmium Phases, Acta Metall. 11 (1963) p 427-434.
[38] P. Herasymenko, Thermodynamic Properties of Solid Solutions, Acta Metall. 4(1) (1956) p 1-6.
[39] D.B. Masson and J.L. Sheu, Variations in the Composition Dependence of the Activity Coefficient in Terminal Solid Solutions of Ag-Zn, Ag-Cd, and Cu-Zn, Metall. Trans. 1(11) (1970) p 3005-3009.
[40] G. Scatchard and R.H. Boyd, The Equilibrium of α -Silver-Cadmium Alloys with

Cadmium Vapor, J. Am. Chem. Soc. 78 (1956) p 3889-3893.
[41] E.J. Rapperport and J.P. Pemsler, Thermodynamic Measurements using Atomic Absorption, Trans. Met. Soc. AIME 242 (1968) p 151-152.
[42] C.E. Birchenall and C.H. Cheng, The Vapor Pressures of Zinc and Cadmium over some of their Silver Alloys, J. Met. 185 (1949) p 428-434.
[43] A. Olander, Eine Elektrochemische Untersuchung von Cadmium-Silber Legierungen, Z. Phys. Chem. A163 (1933) p 107-121.
[44] O.J. Kleppa, Heat of Formation of Solid and Liquid Alloys in the Systems Silver-Cadmium, Silver-Indium, and Silver-Antimony at 450°, J. Phys. Chem. 60 (1956) p 846-852.
[45] J. Waldman, A.K. Jena and M. Bever, Trans. Met. Soc. AIME 245 (1969) p 1039-1043.
[46] R.L. Orr, A. Goldberg and R. Hultgren, Heats of Formation of α-Phase Silver-Cadmium Alloys, J. Phys. Chem. 62 (1958) p 325-327.
[47] P.D. Anderson, The Thermodynamic Properties of the Silver-Cadmium System, J. Am. Chem. Soc. 80 (1958) p 3171-3175.
[48] A. Schneider and H. Schmid, Die Dampfdrucke des Zinks und Cadmium uber ihren Binaren Flussigen Legierungen mit Kupfr, Silber und Gold, Z. Elektrochem., 48(11) (1942) p 627-639.
[49] W. Van Gool, Neth. Koninkl. Ned. Akad., Wentenschap. Proc. 66 (1963) Ser. B4, p 209-215.
[50] D.R. Conant and H.S. Swofford, Solute-Solvent Interactions in Liquid Alloys, J. Chem. Eng. Data 14(3) (1969) p 369-372.
[51] V.N. Volodin, V.E. Khrapunov, B.K. Kenzhaliev, R.A. Isakova, M. Moldabaev, Thermodynamic Study of the Silver-Cadmium System with Determination of the Upper Boundary of Existence of Liquid Alloys, Russ. J. of Non-Ferrous Metals, 46(5) (2005) p 15-22.
[52] R.A. Schaeffer and F. Hovorka, Electromotive-Force Measurements of Molten Binary Alloys, J. Electrochem. Soc. 87(23) (1945) p 267-286.
[53] B.L. Houseman and D.R. Conant, Cadmium Activities of Silver-Cadmium Alloys Determined from Measurements on EMF Cells Involving Displacement Reactions, High Temp. Sci., 1984, 17, p 251-265.
[54] T. Gomez-Acebo, Thermodynamic Assessment of the Ag-Zn System, CALPHAD, 22(2) (1998) p 203-220.
[55] M. Kowalski and P.J. Spencer, Thermodynamic Reevaluation of the Copper-Zinc System, J. Phase Equilib. 14(4) (1993) p 432-438.
[56] R. Schmid-Fetzer, B. Hallstedt, Is zinc HCP_ZN or HCP_A3?, CALPHAD 37 (2012) p 34-36.
[57] A.T. Dinsdale, SGTE data for pure elements, CALPHAD 15(4) (1991) p 317-425.
[58] J.E. Saal, S. Kirklin, M. Aykol, B. Meredig, C. Wolverton, Materials Design and Discovery with High-Throughput Density Functional Theory: The Open Quantum Materials Database (OQMD), JOM 65 (2013) p 1501-1509.
[59] F. Weibke and H.Eggers, The Ag-In System, Z. Anorg. Allg. Chem. 222 (1935) 145-160.
[60] W. Hume-Rothery, G.W. Mabbott and M. Channel-Evans, The Ag-In System, Philosophical Transactions of the Royal Society (London) A(233) (1934) p 1-97.
[61] W. Hume-Rothery and P.W. Reynolds, The Ag-In System, Philos. Trans. R. Soc. London A(160) (1937) p 282-303.
[62] E.A. Owen, E.W. Roberts, Factors Affecting the Limit of Solubility of Elements in Copper and Silver, Phil. Mag. 27 (1939) p 294-327.

[63] E. Hellner, The Binary System Silver-Indium, Z. Metallkd. 42 (1951) p 17-19.
[64] M.E. Straumanis and S.M. Riad, Trans. Am. Inst. Min., Metall. Pet. Eng. 233(5) (1965) p 964-967.
[65] H.J. Snyder, Primary Solid-Solution Phase Boundary in Silver Corner of Silver-Cadmium-Indium Ternary System, Trans. Met. Soc. AIME 239 (1967) p. 1385-1391.
[66] A.N. Campbell and R. Wagemann, and (in part) R. B. Ferguson, The Silver-Indium System: Thermal Analysis, Photomicrography, Electron Microprobe, and X-ray Powder Diffraction Results, Can. J. Chem. 48 (1970) p 1703-1715.
[67] Z. Bahari, J. Rivet, B. Legendre and J. Dugué, Study of the Ag–In–Te ternary System, II. Description of the Quadrilateral Ag–Ag2Te–In2Te3–In, J. Alloys Compd. 299 (1999) p 99-115.
[68] R.L. Orr and R. Hultgren, Heats of Formation of α Phase Silver-Indium Alloys, J. Phys. Chem. 65 (1961) p 378-380.
[69] C.B. Alcock, K.T. Jacob and T. Palamutcu, Thermodynamics of □-Solid Solutions of Silver with Indium and Tin, Acta Metall. 21(7) (1973) p 1003-1009.
[70] D.B. Masson and S.S. Pradhan, Measurements of Vapor Pressure of Indium over α Ag-In Using Atomic Absorption, Metall. Trans. 4 (1973) p 991-995.
[71] K. Itagaki, A. Yazawa, Measurements of Heats of Mixing in Liquid Silver Binary Alloys, J. Jpn Inst. Met. 32 (1968) p1294-1300.
[72] R. Beja and M. Laffitte, C.R. Acad. Sci., Paris (1968), 267 C,123, and R. Beja, reported by [73] as private communication.
[73] R. Castanet, Y. Claire and M. Laffitte, Propriétés Thermodynamiques des Solutions Liquides Argent-Indium, J. Chim. Phys. Phys.-Chim. Biol. 67(4) (1970) p 789-793.
[74] A. Sabbar, A. Zrineh, J.P. Dubès, M. Gambino, J.P. Bros and G. Borzone, The Ag-Bi-In system: Enthalpy of Formation, Thermochim. Acta 395 (2003) p 47-58.
[75] C.B. Alcock, R. Sridhar and R.C. Svetberg, A Mass Spectrometric Study of the Binary Liquid Alloys, Ag-In and Cu-Sn, Acta Metall. 17 (1969) p 839-844.
[76] G. Qi, M. Hino and T. Azakami, Thermodynamic Study of Liquid Ag-In and Ag-Ga Alloys with a Knudsen Cell-mass Spectrometer, Mater. Trans., JIM 30 (1989) p 575-582.
[77] E. Przezdziecka-Mycielska, J. Terpilowski and K. Strozecka, Thermodynamic Properties of Liquid Metallic Solutions XI. The Ag-In System, Arch. Hutn., 8 (1963) p 85-102.
[78] T. Nozaki, M. Shimoji and K. Niwa, Thermodynamic Studies on Liquid Silver-Indium Alloys, Trans. Jpn. Inst. Met. 7(52) (1966) p 52-55.
[79] K. Kameda, Y. Yoshid and S. Sakairi, Activities of Liquid Silver-Indium Alloys by EMF Measurements Using Zirconia Solid and Fused Salt Electrolytes, J. Jpn. Inst. Met. 45(6) (1981) p 614-620.
[80] D. Jendrzejczyk and K. Fitzner, Thermodynamic Properties of Liquid Silver–Indium Alloys Determined from e.m.f. Measurements, Thermochim. Acta 433 (2005) p 66-71
[81] B. Predel and U. Schallner, Untersuchung der thermodynamischen Eigenschaften flussiger binaren Legierungen des Silbers und Goldes mit Gallium, Indium und Germanium, Z. Metallkd. 63 (1972) p 341-347
[82] P.Y. Chevalier and E. Fischer, XXIIièmes Journées d'Etude des Equilibres entre Phases, 15-16 Avril 1996,Toulon, France.
[83] P.-Y Chevalier and E. Fischer, unpublished assessment, Thermodata, 2001.
[84] Landolt-Bornstein, "Thermodynamic Properties of Inorganic Materials", Group IV, vol.19, Subvolume B, Part 1, Springer-Verlag Berlin Heidelberg (2005).
[85] W. Gierlotka, Thermodynamic Description Of The Quaternary Ag-Cu-In-Sn System , J. Electron. Mater. 41(1) (2012) p 86-108.

[86] T.M. Korhonen and J.K. Kivilahti, Thermodynamics of the Sn-In-Ag Solder System, J. Electron. Mater., 27(3) (1998) p 149-158.
[87] H. Okamoto, Ag-In (Silver-Indium) J. Phase Equilibria and Diffusion 27(5) (2006) p 536-537.
[88] S. Curtarolo et al., AFLOWLIB.ORG: A Distributed Materials Properties Repository from High-Throughput Ab Initio Calculations, Comp. Mat. Sci. 58 (2012) p 227-235.
[89] T. Heumann and B. Predel, The Phase Diagram Indium-Cadmium, Z. Metallkd. 50 (1959) p 309-314, and Observations on the conversion of cubic and tetragonal phase in indium-cadmium mixed crystals and the resulting conversion plasticity, Z. Metallkd. 53 (1962) p 240-245, in German
[90] A. Rosina, Determination of Thermodynamic Activities in System Cd-In by Calorimetric Measurements, Rud.-Met. Zb. 2(3) (1971) p 85-105.
[91] D.A. Petti, Silver-Indium-Cadmium Control Rod Behaviour in Severe Reactor Accidents, Nucl. Technol. 84 (1989) p 128-151.
[92] B. Bowsher, A. Jenkins, A. Nichols and N. Simpson, JAH, UKAEA Rep. AEEW-R, (1991).
[93] P. Jones, Third Yr Project Report, University of Manchester, Materials Science Centre (1991).
[94] J. Robinson, Third Yr Project Report, University of Manchester, Materials Science Centre (1991).
[95] A. Decreton, Contribution Expérimentale à l'Etude Thermodynamique des Systèmes Ag-Zr et Ag-Cd-In, Thesis, Université d'Aix-Marseille-IRSN (2016).
[96] C. Desgranges, "Compréhension et prédiction du comportement sous irradiation neutronique d'alliages absorbants à base d'argent", rapport CEA-R-5805 (1998)
[97] B. Cheynet, P.-Y. Chevalier, and E. Fischer, Thermosuite, CALPHAD 26(2) (2002) p 167–74. doi:10.1016/S0364-5916(02)00033-0.